16th Euroseminar on Microscopy Applied to Building Materials

EMABM 2017

14-15-16-17 May 2017
Les Diablerets, Switzerland

emabm2017.epfl.ch

Euroseminars on Microscopy Applied to Building Materials

EMABM

ÉCOLE POLYTECHNIQUE FÉDÉRALE DE LAUSANNE

Disclaimer

HYDROTALCITE AND M-S-H IDENTIFICATION IN 19TH CENTURY ROMAN CEMENT MORTARS

C. Gosselin [1], S. B. Feldman [2]

[1] *Geotest SA, Switzerland.* [2] *National Institute of Standards and Technology, USA*

Introduction

Historic Roman cement (RC) mortars are frequently seen in civil engineering and architectural structures built in the 19th century. Their application (stone compatibility in restoration or concrete, render and cast elements in new buildings) and sound performance in different environments (urban, marine, underground exposure) have made them known for being durable and long-lasting cementitious materials. Roman cements are processed from the calcination of clay-rich marlstones in shaft kilns at temperatures of 800 °C to 1200 °C. Despite the variation in composition due to the local raw materials and uneven calcination conditions, the hydraulic reactivity of RCs usually lies between that of highly hydraulic lime and Portland cement, with a predominance of the Ca-Si-Al system in the amorphous and crystalline phases involved in hydration process [1,2]. Other minerals, such as anhydrite ($CaSO_4$), can be present in some modern RCs (*e.g.*, Rosendale in the US, Vicat in France) [2,3] and significantly change the hydration process by the formation of SO_3-AFm/AFt phases. The samples studied here are joint and filling mortars used to build a railway tunnel in the mid-1870s in Lausanne, Switzerland. The nature of this cement is very unusual and strongly different than other contemporary 19th century RCs in that magnesium is identified in appreciable amounts and within different mineralogical phases, including both residual phases in primary cement grains and in hydration products.

Case study, samples and methods

The tunnel of Montbenon in Lausanne, Switzerland, dates from 1875 to 1877 [4]. The underground railway (Chemin de Fer Lausanne-Ouchy) was built to link the main train station to upper neighbourhoods of Lausanne. The local rock is dominated by sandstone but the tunnel was mostly manually excavated in a compact layer of glacial till (clay or sand, depending on the height of excavation). The structure of the tunnel is composed of 100 rings (2.5 m long, ~6.0 m of final height from the rails level), each successively built with a vertical shift of 0.3 m to ensure a slope of about 12% over the total length of 253 m. The average thickness of each ring is 0.65 m at the vault level and 0.9 m at the foot level. Each ring was built independently, with no mechanical bond between rings according to the Belgium process (the vault was built first and then the vertical feet at last). The masonry is composed of local limestone ashlars jointed by RC mortar. The gaps between the rock and the masonry rings are filled with mortars mixed with fragments of limestone to ensure the structural stability and to make the structure as waterproof as possible. The current state of conservation of the masonry is good even though local areas of water leakage and calcium carbonate concretions are observed through the vaults section. A recent survey campaign allowed five samples (labelled C1-1, C1-2, C2, C3-1 and C3-2) to be collected all along the tunnel, in vault and foot sections. These mortar samples were manually ground to less than 100 μm for the x-ray powder diffraction (XRD) analyses that were carried out with an *X'Pert* Pro PANalytical[1] diffractometer (CuK, λ=1.54 Å). Bulk samples were impregnated with epoxy resin and polished to obtain cross sections to study the microstructure with Scanning Electron Microscopy (SEM, Philips Quanta 200[1]) and Energy Dispersive Spectroscopy (EDS, Bruker AXS Quantax[1]).

XRD Rietveld results

Rietveld quantification of the five samples shows that the sand fractions are principally comprised of calcite, quartz, muscovite, albite, kaolinite, microcline and chlorite in comparable amounts among all samples (Table 1). Moderate amounts of gehlenite were also present as an unreacted crystalline cement phase in two samples. The phases related to the cement hydration are hillebrandite, brucite and hydrotalcite. Hillebrandite, $Ca_2SiO_3(OH)_2$, is a natural member of the CaO-SiO_2-H_2O ternary system which has been previously reported and compared to other wollastonite-types of synthetic C-S-H phases present in Portland cements [5,6]. Brucite, $Mg(OH)_2$, is usually reported in Portland cement concrete exposed to magnesium salts (*e.g.,* sea water, magnesium sulfate), as ion exchange between Mg^{2+} and Ca^{2+} in $Ca(OH)_2$. Beside the durability issues, MgO is predicted to precipitate in Portland cement initially as brucite and later to convert to hydrotalcite if the pore solution is free of sulphate [7]. In the present samples, hydrotalcite is clearly identified and quantified (8 to 14

[1] Certain commercial products are identified in this paper to specify the materials used and procedures employed. In no case does such identification imply endorsement or recommendation by the National Institute of Standards and Technology, nor does it indicate that the products are necessarily the best available for the purpose.

wt% of the crystalline fraction) with the structure $Mg_{5.4}Al_{2.6}(CO_3)_{1.3}(OH)_{16}.4(H_2O)$.Hydrotalcite is reported in the hydration of ordinary Portland cement (OPC) systems (SO_3-free pore solution, see above [7]) and generally as a slag hydration product in alkali-activated-slag and blended systems [8,9].

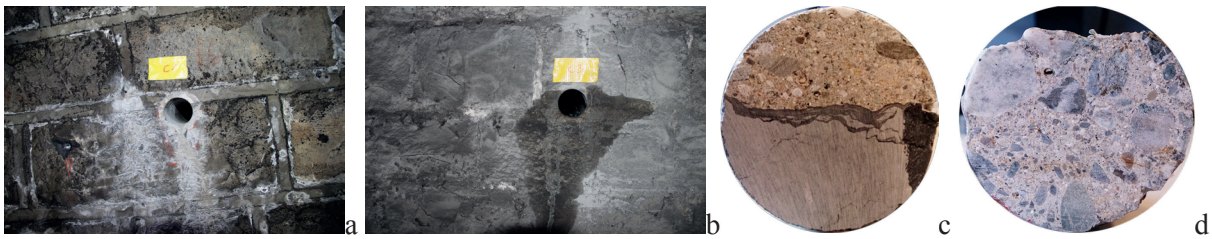

Figure 1 Surface of the masonry (local soiling, leaching and calcium carbonate efflorescence) and the location of the cores (a: C1 vault, b: C3 vertical foot). Cross sectional view of the samples (c: C1, d: C3)

Table 1. XRD Rietveld quantification of the mortars samples

	C1-1	C1-2	C2	C3-1	C3-2
Calcite	45.5	45.3	35.6	32.3	43.1
Quartz	20.4	23.9	24.3	27.9	24.8
Muscovite	4.4	4.0	1.9	5.0	4.8
Albite	3.0	4.2	5.7	5.7	6.8
Gehlenite	3.0	2.4	tr	--	--
Dolomite	1.8	3.3	0.5	0.7	--
Aragonite	3.0	--	2.5	--	--
Hydrotalcite	11.0	8.2	14.8	13.9	7.9
Kaolinite	1.4	2.0	2.1	1.9	3.3
Microcline	3.3	3.0	5.0	4.1	3.7
Hillebrandite	1.8	1.7	--	--	--
Brucite	--	--	6.5	3.2	--
Chlorite	1.6	2.0	1.2	2.4	3.1
Tilleyite	--	--	--	3.0	2.6
Sum	100.2	100.0	100.1	100.1	100.1

SEM results

The microstructure of the mortar has a relatively low density as a result of both low compaction in the fresh state and a low cement-to-aggregates volume ratio. Numerous pores and cavities are observed through the matrix, but the interface and bond with the structural limestone and aggregates are relatively strong (Figure 1c and Figure 2a). Two principal groups of cement grains can be differentiated. The first group (Figure 3a) is related to the grains produced at moderate temperature of calcination (about 800 °C to 1000 °C). These grains are partially dissolved but remaining raw materials (calcium carbonate, quartz, feldspar) are observed. This type of residual material is very common in historic and modern Roman cements [1,2,10]. In contrast, Group 2 grains are comprised of different crystalline phases formed at higher temperatures reached locally in the shaft kilns. This group is illustrated in Figure 3b, showing the complex microstructure of a coarse cement grain.

The easily identified phases of the second group originating from the raw materials (calcium carbonate, kalsilite $KAlSiO_4$ as a temperature conversion product of kaolinite) are not consumed during the calcination. Various phases containing magnesium are present, but the exact determination of their composition is challenging by EDS only. The first phase, labelled M_1, has an atomic composition of $Ca_{16}Mg_6Si_{15}Al_{2.5}O_{58}$ and could be a solid solution of the melilite group (with end-members åkermanite $Ca_2Mg[Si_2O_7]$ and gehlenite $Ca_2Al[AlSiO_7]$) as commonly reported in slag [11]. A second Mg-bearing phase, M_2, has a wt% composition of $Mg_{33}Si_{19}O_{47}$, close to that of forsterite Mg_2SiO_4, the Mg-rich end-member of the olivine series. The phase M3 is a complex solid solution containing Mg-Al-Fe (11 at% each component) and Ti-Ca-Si (2 to 3 at% each component). Finally, the darker phase labelled F is a solution with an atomic composition $Si_{26}Al_{4.5}K_3O_{63}$. Even though the composition fits with that of a member of the feldspar group, this phase has a variable backscattered electron (BSE) density within the grain, which could possibly indicate exsolution or a weathering pattern. Here

the limitations of SEM-EDS are reached and complementary optical microscopy could be useful to better characterize this phase.

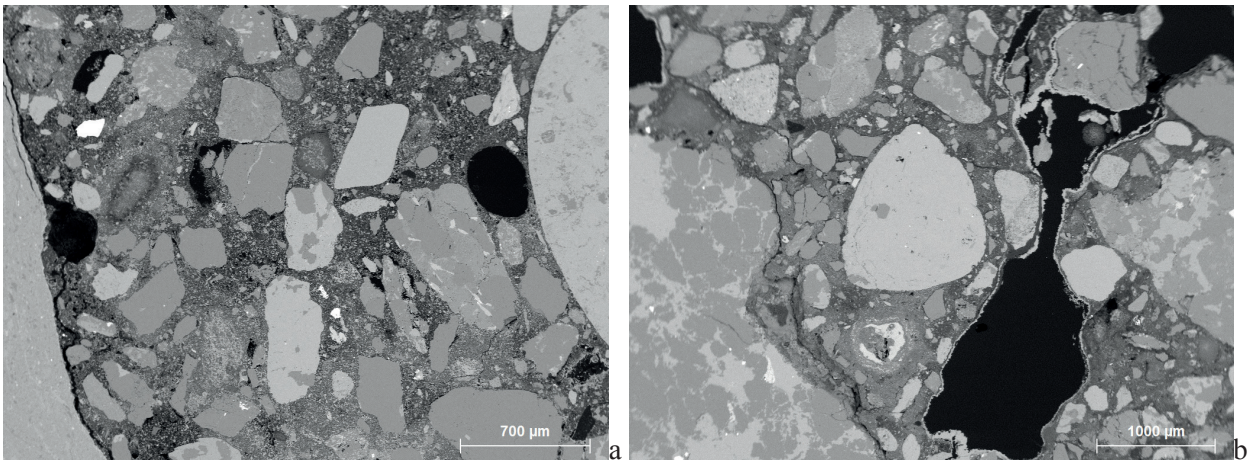

Figure 2 Overall microstructure of the C1-1 sample (a) with poorly packed matrix and sound interface with the structural limestone (left) and the aggregates (center and right). Microstructure of the C3-1 sample (b) with numerous pores coated with leaching products.

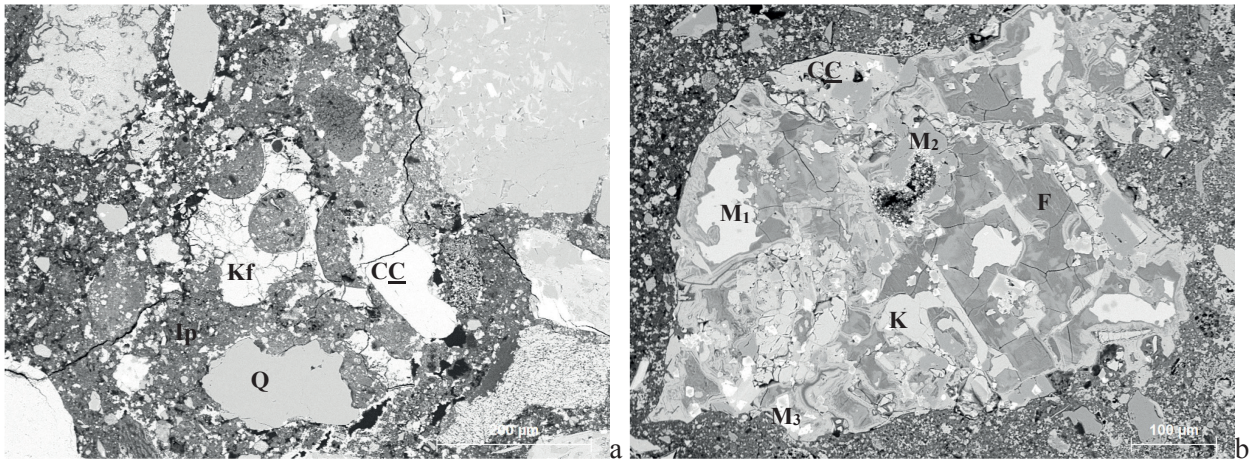

Figure 3 Group 1 grain (a), with amorphous and remaining raw phases (CC calcium carbonate, Q quartz, Kf K-feldspar related $K_{13}Al_{13}Si_{27}O_{47}$ in wt%, Ip inner hydration products), Group 2 grain (b) with crystalline phase (CC calcium carbonate, K kalsilite, M_1, M_2, M_3 magnesium bearing phases described in the text, F see text)

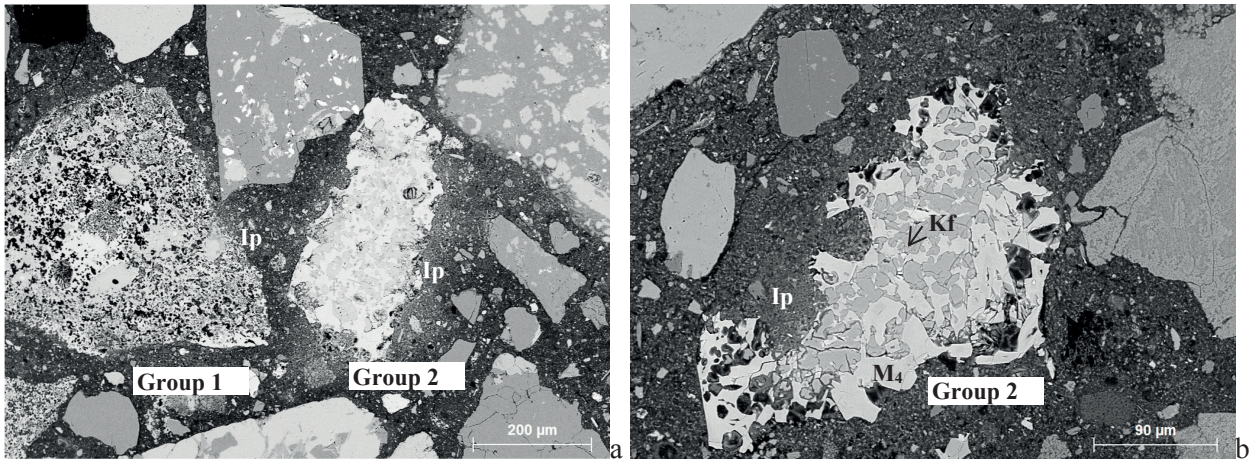

Figure 4 Hydration products of cement grain Group 1 and 2: sample C1-2 (a), sample C1-3 (b, Kf K-feldspar related $K_{13}Al_{13}Si_{27}O_{47}$ in wt%, M4 magnesium solid solution $Mg_7Al_6Si_{20}Ca_{17}Fe_6O_{43}$ in wt%, Ip inner hydration products)

The hydration products are evenly distributed but show different BSE grey levels (Figure 4a). The composition of the inner hydration products, measured at the very boundary of the cement grains of both type 1 and 2 (Figure 4), is characterized by the dominance of magnesium present in both M-S-H and hydrotalcite-type phases, as illustrated by the atomic ratio plots of Figure 5, measured over different samples and group of cement grains.

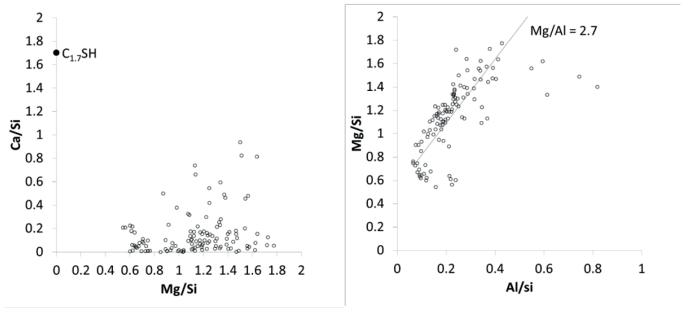

Figure 5 Ca/Si vs Mg/Si and Mg/Si vs Al/Si plots of the inner hydration products

Conclusions

In contrast to usual RCs, the present samples do not show any residues of C_2S and any signifiant quantities of C-(A)-S-H and AFm phases. Although the XRD analysis indicates the presence of C-S-H (identified as crystalline hillebrandite) as primary hydration products, SEM reveals the predominance of amorphous M-S-H with 0.6 <Mg/Si< 1.5. The measured atomic Mg/Si ratio is comparable to that of M-S-H studied in activated slag systems [8,12]. In this study the formation of M-S-H is understood as a reaction product between the decalcified primary C-S-H (driven by water percolation through the structure) and available Mg in the pore solution. Magnesium is likely progressively dissolved by the different cement phases (*e.g.,* forsterite, Mg_2SiO_4, and the different solid solutions described above). Besides their contribution to the formation of M-S-H, the Mg-bearing phases directly hydrate to hydrotalcite-type phases identified by both XRD and EDS, with a ratio Mg:Al = 2.7, lying between that of quintinite (2:1) and hydrotalcite (3:1) as reported in hydrotalcite-type in slag systems [13]. The formation of M-S-H does not appear to be related to any microstructure degradation.

REFERENCES

[1] F. Pintér, I. Vidovszky, J. Weber, K. Bayer, Mineralogical and microstructural characteristics of historic Roman cement renders from Budapest, Hungary, J. Cult. Herit. 15 (2014) 219–226.

[2] C. Gosselin, K.L. Scrivener, S.B. Feldman, W. Schwarz, The hydration of modern Roman cements used for current architectural conservation, in: Hist. Mortars, Springer, 2012: pp. 297–308.

[3] R. Vyskocilova, W. Schwarz, D. Mucha, D. Hughes, R. Kozłowski, J. Weber, Hydration processes in pastes of Roman and American natural cements, J ASTM Int. 4 (2007).

[4] E. Cuénod, Notice sur les travaux du tunnel de Montbenon à Lausanne, Bull. La Société Vaudoise Des Ingénieurs Des Archit. 1 (1875) 21–23.

[5] I.G. Richardson, The calcium silicate hydrates, Cem. Concr. Res. 38 (2008) 137–158.

[6] Yongshan Dai, J.E. Post, Crystal structure of hillebrandite: a natural analogue of calcium silicate hydrate (CSH) phases in Portland cement, Am. Mineral. 80 (1995) 841–844.

[7] B. Lothenbach, F. Winnefeld, Thermodynamic modelling of the hydration of Portland cement, Cem. Concr. Res. 36 (2006) 209–226.

[8] X. Ke, S.A. Bernal, J.L. Provis, Controlling the reaction kinetics of sodium carbonate-activated slag cements using calcined layered double hydroxides, Cem. Concr. Res. 81 (2016) 24–37.

[9] M. Whittaker, M. Zajac, M. Ben Haha, F. Bullerjahn, L. Black, The role of the alumina content of slag, plus the presence of additional sulfate on the hydration and microstructure of Portland cement-slag blends, Cem. Concr. Res. 66 (2014) 91–101.

[10] C. Gosselin, Composition and Hydration of some Roman (natural) Cements, in: The Institute of Concrete Technology Yearbook 2013-2014, 18th ed., London, 2013: pp. 64–72.

[11] F. Engström, D. Adolfsson, C. Samuelsson, Å. Sandström, B. Björkman, A study of the solubility of pure slag minerals, Miner. Eng. 41 (2013) 46–52.

[12] S.A. Walling, J.L. Provis, Magnesia-Based Cements: A Journey of 150 Years, and Cements for the Future?, Chem. Rev. 116 (2016) 4170–4204.

[13] R. Taylor, I.G. Richardson, R.M.D. Brydson, Composition and microstructure of 20-year-old ordinary Portland cement-ground granulated blast-furnace slag blends containing 0 to 100% slag, Cem. Concr. Res. 40 (2010) 971–983.